

CRITICAL REVIEW

From theory to practical fundamentals of electroencephalographic source imaging in localizing the epileptogenic zone

Jaysingh Singh¹  | John S. Ebersole² | Benjamin H. Brinkmann^{3,4} 

¹Department of Neurology, The Ohio State University Wexner Medical Center, Columbus, Ohio, USA

²Northeast Regional Epilepsy Group, Atlantic Health Neuroscience Institute, Summit, New Jersey, USA

³Department of Neurology, Mayo Clinic, Rochester, Minnesota, USA

⁴Department of Biomedical Engineering, Mayo Clinic, Rochester, Minnesota, USA

Correspondence

Jaysingh Singh, Department of Neurology, Wexner Medical Center, Ohio State University, Columbus, OH, USA.

Email: dr.jaysingh@hotmail.com

Benjamin H. Brinkmann, Department of Neurology, Mayo Clinic, Rochester, MN, USA.

Email: brinkmann.benjamin@mayo.edu

Abstract

With continued advancement in computational technologies, the analysis of electroencephalography (EEG) has shifted from pure visual analysis to a noninvasive computational technique called EEG source imaging (ESI), which involves mathematical modeling of dipolar and distributed sources of a given scalp EEG pattern. ESI is a noninvasive phase I test for presurgical localization of the seizure onset zone in focal epilepsy. It is a relatively inexpensive modality, as it leverages scalp EEG and magnetic resonance imaging (MRI) data already collected typically during presurgical evaluation. With an adequate number of electrodes and combined with patient-specific MRI-based head models, ESI has proven to be a valuable and accurate clinical diagnostic tool for localizing the epileptogenic zone. Despite its advantages, however, ESI is routinely used at only a minority of epilepsy centers. This paper reviews the current evidence and practical fundamentals for using ESI of interictal and ictal epileptic activity during the presurgical evaluation of drug-resistant patients. We identify common errors in processing and interpreting ESI studies, describe the differences in approach needed for localizing interictal and ictal EEG discharges through practical examples, and describe best practices for optimizing the diagnostic information available from these studies.

KEYWORDS

EEG source imaging, electrical source imaging, epileptogenic zone, head model, inverse model

1 | INTRODUCTION

The success of epilepsy surgery depends on accurate localization of epileptogenic zone (EZ), which is defined as brain regions involved in seizure onset and initial propagation that need to be removed to stop seizures.^{1,2} Over the past decade, there has been a dramatic increase in National Association of Epilepsy Centers (NAEC)-approved epilepsy centers providing comprehensive

surgical evaluation, from 133 centers in 2011 to 261 centers in 2021 (NAEC Webinar, April 6, 2021). Presurgical phase I assessment for most of the epilepsy centers includes visual analysis of interictal–ictal electroencephalographic (EEG) data, magnetic resonance imaging (MRI), positron emission tomography (PET), and single photon emission computed tomography (SPECT), which guides their decision in selecting patients for surgical evaluation, and planning strategies for intracranial monitoring and

This is an open access article under the terms of the [Creative Commons Attribution-NonCommercial](https://creativecommons.org/licenses/by-nc/4.0/) License, which permits use, distribution and reproduction in any medium, provided the original work is properly cited and is not used for commercial purposes.

© 2022 The Authors. *Epilepsia* published by Wiley Periodicals LLC on behalf of International League Against Epilepsy.

cortical resection. Undoubtedly, MRI, PET, and SPECT are valuable imaging tools that could help localize the EZ in 50%–80% of cases, depending on the presence or absence of lesion.^{2–4} Similarly, conventional 32-channel EEG is a valuable tool to classify the epileptic syndrome, but the overall sensitivity and specificity of visual analysis of scalp EEG epileptic spikes to localize the EZ are low, especially in the absence of structural lesion and in extratemporal lobe onset epilepsy.

EEG source imaging (ESI) is an inexpensive and noninvasive clinical diagnostic tool that integrates temporal and spatial components of EEG to localize the sources of given interictal and ictal scalp EEG signals in real time. With an adequate number of electrodes combined with patient MRI-based head models, ESI can localize the epileptic focus with up to 88% specificity and 84% sensitivity, which is higher than MRI or PET brain imaging.⁵ Although the principles of signal detection, signal analysis, and source localization for EEG are quite similar to magnetoencephalography (MEG), ESI is found to be more sensitive in localizing the radial sources from gyral cortical planes, which are rich in corticocortical connections, pyramidal arborization, and cortical laminations and account for most of the human cortical homunculus.^{6,7} Other practical advantages of ESI over MEG include feasibility in the pediatric age group and using ictal studies for source localization. A comprehensive review by Plummer et al. in 2008 suggested that ESI should be incorporated into the routine presurgical assessment.⁸ However, only one third of epilepsy centers were found to be using ESI in surgical assessment.⁹ This is likely an outcome of multiple factors, which include lack of training with advanced EEG signal analysis during fellowship training, difficulty with using high-density (HD) electrodes and image coregistration, and low reimbursement, and also strongly influenced by the strength of the epilepsy program and its habituated pattern of clinical practice.

This review aims to cover the fundamentals behind ESI, and review existing literature evaluating ESI's diagnostic accuracy compared with other structural imaging modalities and ESI's relationship with postsurgical outcomes.

1.1 | Basic principles of ESI

ESI is a promising technique that is rapidly gaining acceptance at epilepsy centers worldwide. Although this technique has the potential to provide high-quality localizing information for ictal and interictal discharges using an inexpensive EEG acquisition and the patient's MRI, a good understanding of the basic concepts and potential pitfalls is essential to ensure appropriate utilization and interpretation of these data. This review is aimed at

Key points

- Modern ESI is a model-based neuroimaging tool that integrates temporal and spatial dimensions of EEG to identify the source of scalp-recorded potentials
- Selection and grouping spikes based on voltage topography and accurate modeling of epileptic spikes are crucial for ESI source localization
- An adequate number of electrodes and using a patient MRI-based realistic head model can dramatically improve the accuracy of ESI
- A hybrid approach of trained personnel reviewing the automated spike detection and source modeling can provide a good alternative to the labor-intensive manual ESI approach

providing both a theoretical understanding of the principles of this technique and practical guidelines for data acquisition, waveform selection, algorithm application, and interpretation of results.

1.2 | Basic concepts of source localization and methodologies

Cortical signals recorded by scalp EEG depend upon a separation of charges arising from postsynaptic membrane potentials in cortical dendrites oriented in parallel columns along the cortex. This parallel orientation allows the dendritic potentials to summate to produce a potential that is detectable by scalp electrodes some distance away, separated by skin, bone, cerebrospinal fluid, and dural tissues. This is an important difference between scalp EEG and invasive EEG—that scalp EEG records distant potentials that are affected by the electrical impedances of intervening tissues, whereas invasive EEG measures local field potentials around neuronal ensembles directly. As such, the neuronal discharges measured by invasive EEG are frequently much higher in amplitude and more spatially constrained around the measuring electrode compared to scalp EEG, which requires a larger ensemble of neurons firing synchronously and in a consistent orientation to be detectable by scalp electrodes. However, invasive EEG suffers from limited spatial sampling, and contacts only record local field potentials very close to the recording electrode. Some debate exists regarding exactly how many cortical columns (i.e., how much cortex) must fire synchronously to produce a measurable potential on the scalp. Experiments using a dry skull phantom and porous dielectric suggested 6 cm² is needed,¹⁰ and simultaneous scalp and cortical EEG recordings have

suggested 10–20 cm².¹¹ However, more recent reports have challenged this figure and suggested this may actually be much lower.¹² Regardless of the exact amount of cortex, scalp-recorded potentials represent the summation of synchronously firing groups of cortical columns, and accurate modeling of the source of the EEG signal should always take this into account. Although similar considerations are involved with MEG source imaging, a realistic volume conduction model may be more important in ESI due to the greater influence of tissue properties on electrical signals than magnetic signals.

1.3 | Equivalent current dipole and current density models

The simplest way to model the source of any separation of electrical charge is using a single point dipole. This form simplifies many of the calculations involved and hence is commonly used in ESI despite its obvious physical inaccuracy. In actuality the inverse problem, where measured voltages at discrete locations on the scalp are used to compute the position, magnitude, and orientation of a source from among a vast number of possibilities, is an ill-posed problem and not analytically solvable, as the possible solutions far outnumber the measured values. The forward problem, however, where scalp voltages are computed based on a particular electrical source and known electrical conductances of tissue, is analytically solvable. In practice, the inverse problem is solved by finding the electrical source using the forward problem that minimizes the mean squared error between the calculated and measured scalp electrical potentials.

Figure 1 illustrates how a potential difference arising from depolarization of parallel cortical columns creates a measured voltage at scalp electrode locations, which are then used to compute an equivalent current dipole solution. Note that due to the distributed nature of cortical depolarization, a single point equivalent dipole must be placed deeper than the actual cortical generator to represent the same distribution of scalp potentials. Furthermore, the depth of the equivalent dipole is proportional to the spatial extent of the cortical sheet generating the potentials.

Current density solutions model the source of the scalp potentials as a spatially distributed array of discrete current sources and use the tissue electrical conductances to compute scalp potentials by solving the forward problem. As with dipole solutions, these sources are estimated iteratively to find the distribution of sources that minimizes the error between the measured scalp potentials and the estimated potentials using the forward model. This tends to be more computationally demanding than dipole solutions, given the multiple contributing cortical sources that

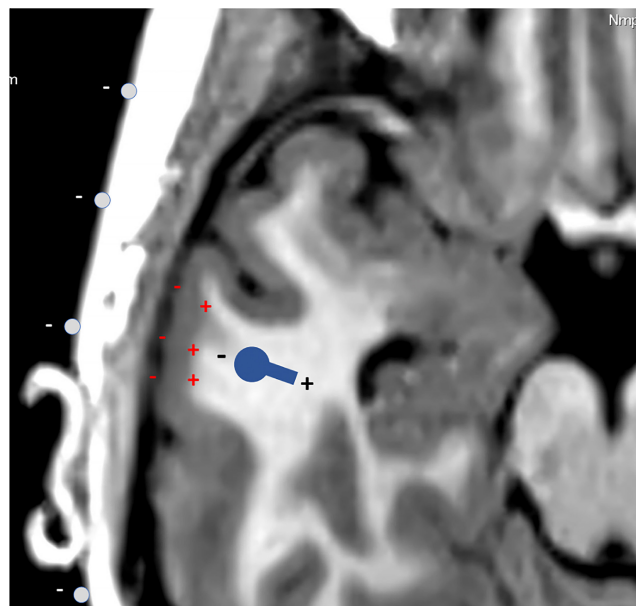


FIGURE 1 Illustration of dipole source estimate.

Depolarization of cortical gray matter generates a local field potential that is measurable by electrodes on the scalp surface. To be measurable on the scalp surface, the region of depolarizing cortex must extend over multiple square centimeters. To represent this spatially distributed depolarization as a single point source, the location of the source must be placed below the actual cortex generating the discharge.

need to be accounted for. The additional degrees of freedom posed by the distributed sources require additional constraints to reach an unambiguous solution. There are several current density approaches that are commonly used and have data from published studies supporting their application to clinical source localization.

Minimum norm is a solution that assumes the dipole distribution and noise vectors are normally distributed with zero mean, and uses the vector pseudoinverse decomposition to identify the solution that minimizes signal power.^{13,14} This is a computationally appealing framework for solving the inverse solution, but minimum norm solutions by themselves tend to bias results toward shallow surface, leading some to use depth-weighted versions of the minimum norm solution.¹⁵

Low-resolution electromagnetic tomography (LORETA) applies a smoothness constraint to the current density solution. There are several variations of LORETA, which involve changes to the basic formulation. Standardized LORETA is very commonly used and has some advantages in stability and accuracy over other formulations.^{16,17} The method can be viewed as a specific instance of a weighted minimum norm solution that maximizes the similarity between adjacent cortical volume elements.¹⁸ LORETA and its variations have been extensively validated using digital simulations and human studies.^{19,20}

The local autoregressive average (LAURA) solution begins with a minimum norm framework but applies Maxwell's equations under the assumption of tissue-specific linear (ohmic) conductances as constraints to generate the inverse solution.²¹ This formulation has the ability to incorporate anatomic or other information by modifying the autoregressive model coefficients. LAURA has been validated in large series²² and has been shown to be robust to brain lesions.²³

It should be noted that these current density models differ from more advanced distributed inverse methods,²⁴⁻²⁶ which simultaneously estimate the location and extent of sources, and are beyond the scope of this review.

1.4 | Interictal discharges

A common approach in ESI is to identify and average multiple interictal epileptiform discharges in the EEG. If the EEG contains a large number of similar discharges, this can be a very

effective method resulting in an averaged signal with a high signal to noise ratio and a reliable localization (see Figure 2).

1.4.1 | Selection of discharges

All focal spikes and/or sharp waves can be source-modeled. Initial selection/identification is usually done by visual inspection of EEG traces as in traditional review. However, this is where the similarity ends. An essential preamble to further analysis is displaying the voltage topography of each sharp transient suspected to be a spike, that is to say, reviewing the voltage field over the entire head, both the negative and positive field maxima. Using subtemporal electrodes bilaterally will be essential in this regard to maximize spatial sampling. True spikes have a dipolar field with smooth gradients between maxima. Artifactual transients usually have a complex, multipolar field with irregular voltage gradients. Field analysis is far more accurate in identifying true

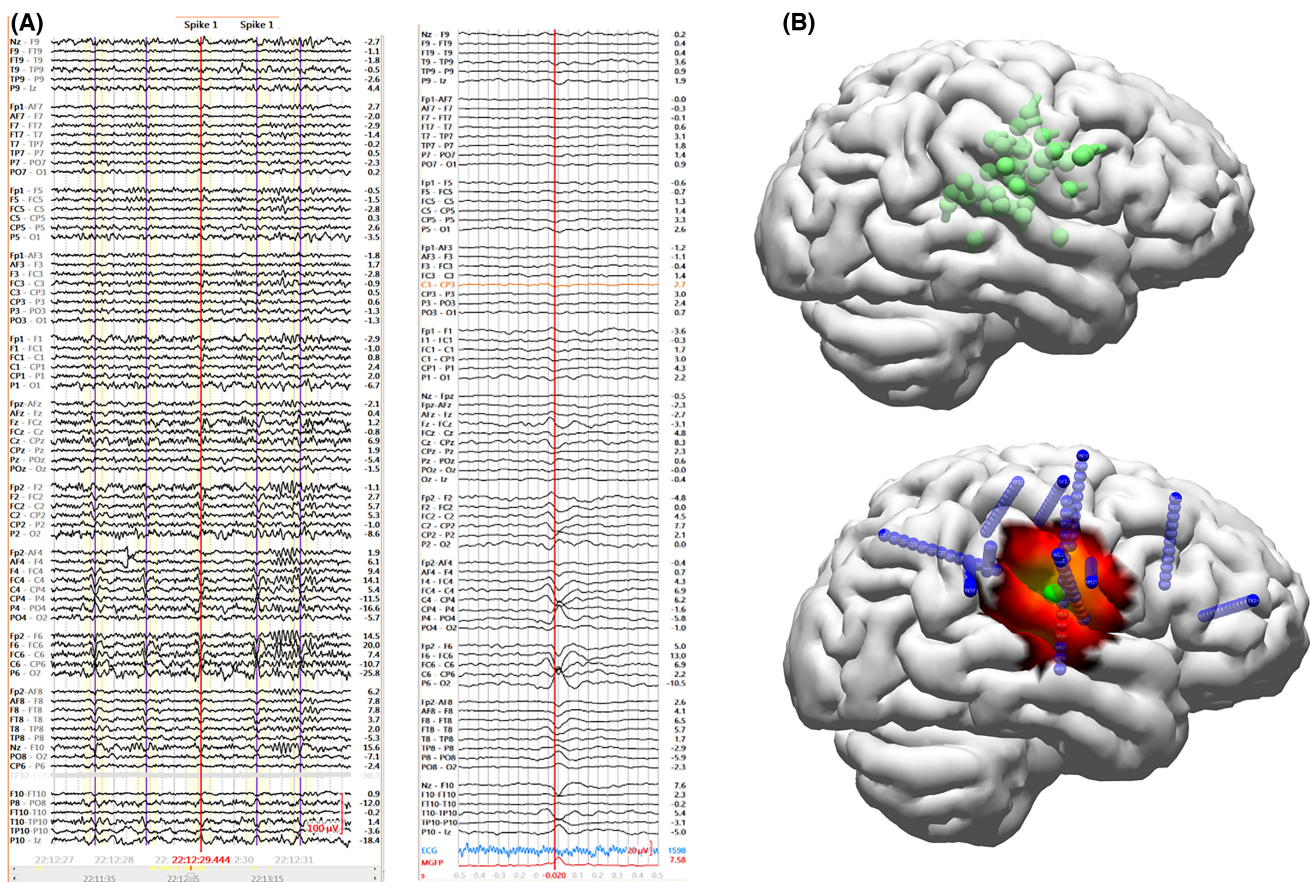


FIGURE 2 Electroencephalographic (EEG) source imaging was performed on a patient with frequent interictal discharges over the right central head region. EEG was recorded using a 76-channel 10–10 electrode array, and numerous interictal discharges were recorded with peak amplitude over FC6. (A) Dipoles were computed for each individual interictal discharge, creating a dipole cluster over the right central head region. (B) The discharges were averaged, improving the signal to noise ratio of the discharge. The discharge was analyzed at approximately 50% of the peak amplitude on the upswing toward the peak using dipole and sLORETA (standardized low-resolution electromagnetic tomography) solutions, localizing the source of the activity to the frontal operculum. Subsequently, stereo EEG monitoring was performed, which showed the onset of seizures to be concordant with the source localization result.

spikes than simply looking at the shape of the EEG transient. This field analysis will also determine the location and strength of both maxima, which is essential for dipole analysis. Importantly, a spike's voltage field will also determine whether its orientation is radial or tangential. Finally, voltage topography over time will reveal whether there is propagation of the generator area to other regions of cortex.

1.4.2 | Segregating spikes into types

This spatiotemporal voltage field analysis is essential in segregating spikes with the same likely generator, as the configuration of the generator cortical source directly determines the voltage topography of the spike. Spike fields with a radial configuration are likely generated by convexity cortex that is parallel to the skull/scalp, whereas tangential spike fields most likely come from sulcal or fissural cortex and certain gyral planes that are oriented perpendicular to the skull. Segregation is typically based on whether the spike field is radial or tangential or between the two (oblique) and the location of the field maxima. For example, a radial spike with a midtemporal negative field maximum would be segregated into a different group or spike type from other temporal spikes with, for example, a tangential field and a frontotemporal (temporal tip) negative field maximum.

1.4.3 | Averaging spikes

Although patients commonly have one predominant spike generator, many have several spike sources. Defining the voltage topography of each spike will segregate those with a similar generator. Spikes also have a variable amplitude and S/N (signal-noise ratio i.e. how much larger they are than background rhythms) (i.e., how much larger they are than background rhythms). By averaging multiple spikes of the same voltage field, one can increase the S/N, which will provide a better substrate for source modeling. It is critical, however, that only spikes of the same topography and evolution over time be averaged together. Commonly one uses an identifiable point on each spike, such as the peak to align the averaging process. This should time lock the source sequence. Any point along the spike can be used for later source modeling. After averaging spikes with all the various fields, one creates a set of spike types that represent each major generator for that patient.

1.4.4 | Dipole modeling

After defining the voltage fields of each spike type, the next goal is to estimate its cortical source within the

brain. As noted in the theoretical discussion of dipole source modeling, this "inverse" solution has no unique answer, given that a number of different source configurations can produce the same scalp field. If one constrains the problem by specifying the number and type of source models to be used and the locations within the head model where they can reside, one can find by computerized and iterative trial and error a dipole location and orientation whose forward solution most closely fits the actual measured field. In the most simple, clinical protocol this will involve finding the best single dipole model within a spherical head model to fit the measured voltage field data. For modern computers, these calculations are fast and easy to make. Several problems with this single dipole solution are obvious. The actual cortical source is not pointlike, but extended over several centimeters, and the head (skull and scalp) is not totally spherical. Source solutions are therefore typically displaced from the actual generator. Accordingly, dipole source models have to be interpreted and cannot be used at face value for clinical decisions.

1.4.5 | Improving dipole source models

Major ways to improve the accuracy of dipole models include using sufficient electrodes to define as well as possible the spike voltage field, making more accurate voltage field measurements, and having a more accurate head model. International 10–20 EEG electrodes cover only the top half of the head. Most spike voltage fields extend into the "southern hemisphere" of the head. Subtemporal electrodes are important for accurate source modeling, particularly of orbitofrontal, temporal base, and inferior occipital sources. Similarly, electrodes are seldom placed exactly in standard 10–20 positions. Measuring in three dimensions the exact electrode locations in an individual patient by any of a number of position digitizing devices is also worthwhile. Finally, the head and skull cavity containing brain are not spherical, particularly along the base. A spherical head model (Figure 3A) will not yield accurate dipoles for these regions. A realistic head model is needed, which can be obtained from volumetric MRI or computed tomographic imaging series by a number of methods. The most popular is the boundary element method and model (boundary element model [BEM]), which tessellates the three-dimensional (3D) surfaces of the inner and outer surfaces of the skull and scalp into thousands of triangles (Figure 3B). Source location calculations using this realistic head model are significantly more accurate for spikes originating in basal head regions. Dipoles from spherical head models are

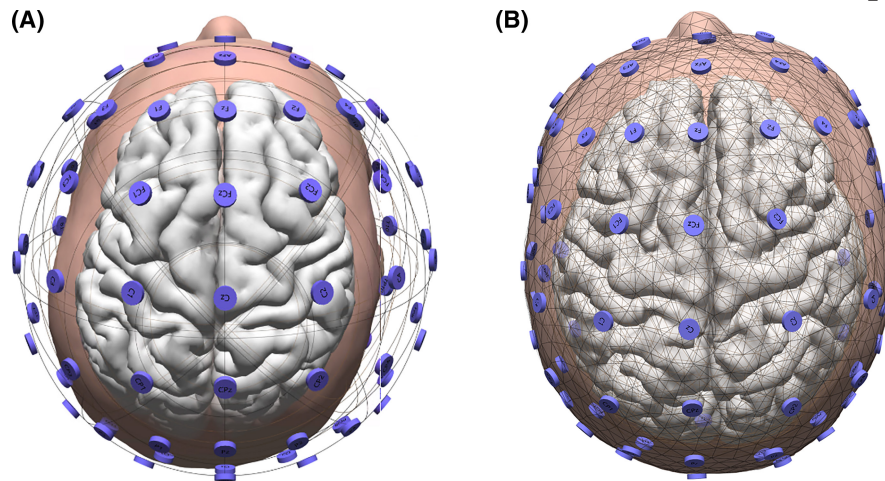


FIGURE 3 Spherical and patient-specific realistic head models. (A) A multicompartment spherical head model can approximate the curvature and shape of the head over the vertex and frontal and occipital regions. However, there is poor correspondence over the lateral and inferior (temporal) head areas. (B) A boundary element model created from the patient's magnetic resonance imaging approximates the shape of tissue surfaces using a mesh of triangular geometric elements, creating a far more accurate representation.

typically ≥ 2 cm higher in the brain than those calculated from BEMs.²⁷ This means, for example, that many dipole models of temporal lobe spikes are misplaced into the frontal lobe.

1.4.6 | Dipole interpretation

Even with all these improvements, pointlike dipole models typically suffer from the problem that they commonly must be deeper than the actual generator cortex to mimic the broad scalp voltage field produced by an extended cortical source. As such, dipoles require clinical interpretation. Their exact location must not be taken as accurate. Therefore, dipole location should not be used for procedures such as stereo EEG (SEEG) trajectory planning. Rather, the interpreted cortical source location should be used.

For most dipole models of spikes with a radial and oblique orientation, the simplest method of interpretation is to extend the dipole vector toward the negative field maximum until it intersects overlying cortex. If the net orientation of that cortex is orthogonal to the dipole, this will be the most likely source. This is easily visualized in a 3D rendering of the brain and dipole by rotating the brain to view the dipole head-on from a perspective above the cortex. The dipole will point to the cortical source. If the dipole is tangential, the source is best defined by also moving the dipole more superficially as well as viewing it head-on. The clearest example of this dual displacement is perhaps dipoles of the temporal lobe base. They commonly lie above the hippocampus, but are really modeling basal cortex.

An additional consideration when mapping interictal epileptiform discharges is the potential for discharges to propagate. Although mapping the discharges at peak amplitude would provide the best signal to noise ratio possible, the peak of the discharge may represent propagation from the discharge's origin, compromising the accuracy of the localization. In theory, localizing the base of the discharge ameliorates any propagation that may have occurred, but this is also the point of lowest signal, and the presence of noise may produce an inaccurate localization.²⁸ The usual solution is to map the discharge at the midpoint of the upswing of the discharge, as this represents a reasonable compromise between these factors. In practice, stable nonpropagating discharges can be mapped at the discharge peak, and starting at the discharge peak and moving the analysis point leftward in steps can be helpful to assess whether the discharge is stationary or propagating.

1.5 | Automated interictal spike detection and modeling

Once the duration of an EEG recording exceeds that of a routine laboratory study, the effort of reviewing it for spikes becomes increasingly burdensome. This is particularly true for long-term monitoring records of several days' duration. Over the past few decades, numerous software programs have been developed to detect spikes and seizures automatically. Early programs depended on various morphological characteristics of sharp and rhythmic transients. Recent software has adopted artificial intelligence (AI) techniques by "teaching" neural networks through

hundreds of examples what a typical spike looks like. Some of these software packages have become very popular and are often offered as part of long-term monitoring (LTM) systems.

Unfortunately, all suffer in some degree from the same deficiency. In order not to miss many real spikes, these programs become too sensitive and also detect many artifacts and normal sharp transients. Many false positives produce decreased specificity, which means that effort must be expended in reviewing the detections and eliminating the false positives. One important improvement in modern spike detection software is the automatic clustering of individual spikes into groups with similar morphology, topological distribution, and/or voltage field. This allows the interpreter to eliminate and or accept entire populations of transients by judging the acceptability of the cluster, rather than reviewing each individual detection.

Several recent publications have compared popular spike detection programs on scalp EEG recordings using LTM results as a gold standard.²⁹⁻³¹ They found high sensitivity for all of them, that is, nearly all true spikes were detected. Unfortunately, all programs also had relatively low specificity (i.e., many false positives). The consensus was that fully automatic spike detection programs, even of the AI type, are not optimal for clinical purposes by themselves. Semiautomated or hybrid approaches, where human interpreters reviewed clusters of spike types and discarded those clusters that did not appear to be spikes, were far superior. Accordingly, it would appear at present that no automated spike (or seizure) detection program is superior to an experienced EEG reader and should not be used alone. Some form of human intervention is needed to increase the specificity and reduce inevitable false positives. Similarly, it goes without saying that dipole or other source modeling of automatically detected spikes makes little sense without human confirmation that the spikes are really epileptogenic. Additionally, it has been found that dipole models from automatically detected spikes are more accurate relative to the surgical resection site if there is a single predominant spike type and if a human interpreter can choose the latency to model (e.g., spike peak or half rising).³¹

However, the clinical objective of spike detection needs to be better defined. On one extreme, is it important to detect as many true spikes as possible to make a quantitative assessment, or on the other, is the goal to determine whether there are any spikes? Perhaps an intermediate position is more realistic, such as identifying the number of spike “types” (i.e., distinct sources), and finding sufficient numbers of each type so that averaging can produce a spike of high S/N for optimal source analysis. This

latter goal would seem to be optimal for the evaluation of patients for possible therapeutic intervention beyond medication.

1.6 | Ictal discharges

Although interictal discharges are a staple of ESI, mapping seizure discharges represents a more direct measure of the seizure onset zone.³² Cortical spikes that are apparent at the scalp typically recruit sufficient adjacent cortex within milliseconds, whereas ictal activity may take seconds to appear on scalp EEG. Ictal onsets are more often corrupted by myogenic artifacts, eye blinks, and other sources of noise. For most patients, prolonged monitoring is required to record seizure discharges, and this carries a greater potential for some channels to lose connection, develop high impedances, and become dominated by inductive noise. Most ESI analysis software allows such channels to be omitted from the localization calculation.

Analysis of seizure onsets require a modified strategy from analysis of interictal discharges. Not all seizure onsets will have adequate scalp representation to provide a reliable result, for example, low-voltage, high-frequency, cerebral seizure onsets are not recognizable at the scalp. Only after some recruitment of adjacent cortex into slower, synchronous activity are scalp ictal potentials visible. Accordingly, it is crucial to seek the earliest recognizable scalp EEG rhythm for source modeling to define the seizure source. Tight band-pass filtering, such as 3–15 Hz for temporal seizures and 3–25 Hz for extratemporal seizures, is often essential in eliminating muscle and movement artifact and in emphasizing the normal scalp ictal frequencies for that brain region. Seizure onsets can be analyzed by selecting the earliest epoch of ictal rhythm and using amplitude-weighted dipole or current density methods. Variations on the single equivalent moving dipole solution are available, and include rotating dipoles and MUSIC (multiple signal classification) dipoles, which use singular value matrix decomposition to model an oscillating source of EEG activity.³³ Independent component analysis is often helpful for removing artifacts and noise that cannot be removed by filtering, including eye blinks and movement artifacts (Figure 4). These algorithms use the spatial and temporal characteristics of the EEG signals to separate the EEG signals into spatiotemporally coherent components, potentially separating different physiological and noise sources. The components can be transformed back into the original signal space with artifact or unwanted signal components zeroed out, reconstructing the original signal without the unwanted features.

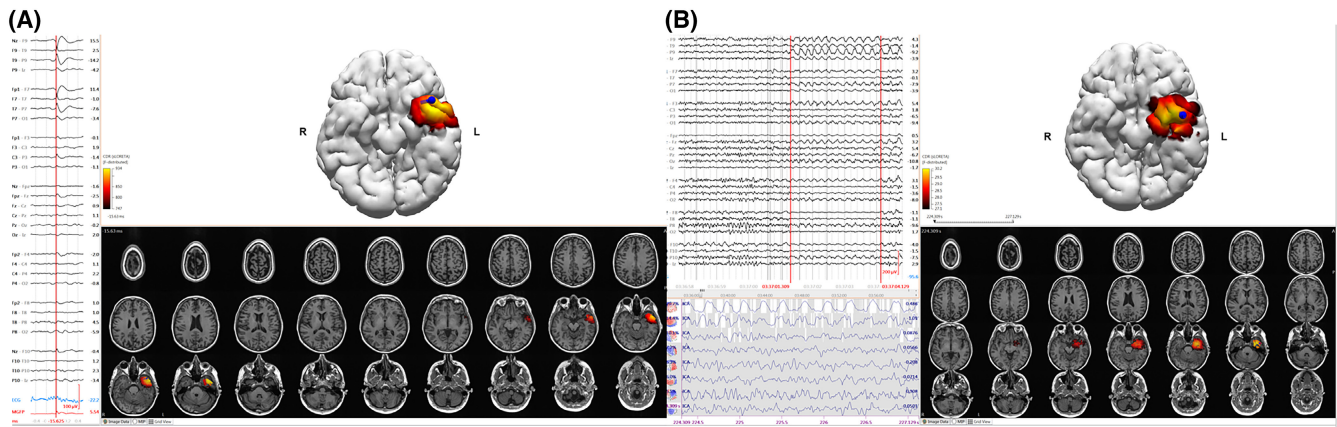


FIGURE 4 (A) Interictal source localization using a 32-channel array recording prolonged electroencephalogram. Interictal spikes with peak amplitude over F9 were averaged, and dipole and standardized low-resolution electromagnetic tomography (sLORETA) solutions localized the source of the discharge to the left temporal pole. (B) Seizure onsets in this patient occur as a theta frequency discharge over F9 and T9. Independent component analysis (ICA) was used to isolate the ictal discharge, seen as the first rhythmic ICA component, from background activity and noise, isolated in the later seven components. MUSIC (multiple signal classification) dipole scan and sLORETA solutions were computed on the first ICA component epoch, and localized the activity to the left temporal pole.

The simplest method to localize a seizure onset is by averaging the peaks of sequential ictal oscillations or spikes after filtration. Here, the same essential principles apply as with interictal discharges. The analysis window may need to be narrowed for theta and other closely spaced discharges, which will influence the algorithm's estimate of signal to noise ratio. In a recent report, Cox et al. showed greater accuracy with a repetitive spiking pattern at onset compared to other patterns.³⁴

Given that the onset of cerebral ictal activity may not be identifiable at the scalp and that recruitment of adjacent cortex into synchronous discharging is likely necessary for a correlate scalp rhythm to appear, dipole and other source models of seizure onset may not localize the initial cortical generator as well as similar models of spikes. A patient is also likely to have spikes with more than one cortical origin. Accordingly, it is reasonable to use the scalp ictal source model to determine the epileptogenic generator lobe and further use spike source models from the same lobar area to refine focus location.

1.7 | Head models

The overall accuracy of the inverse solution depends upon the accuracy of the assumptions and models used in its calculation. This is especially true for the models used to represent the scalp, skull, and brain and their electrical conductances. Early work with ESI was done using idealized spherical head models to reduce computational complexity.^{35,36} These were typically multicompartments models that incorporated measured values of the conductances of tissues. These models often produced moderate

accuracy in the upper half of the head, but rather poor accuracy inferiorly, including the temporal lobes.³⁷ Modern cortex-based head models (Figure 3B) are far more accurate and improve precision in calculating the inverse solution.^{36,38,39,40,41,42} BEMs identify boundaries between tissue types in the brain and model the conductance changes across these boundaries. In contrast, finite element models (FEMs) model tissue volume elements within the cranial compartments, and may provide advantages in more accurately modeling anisotropy and complex geometries, but are also more computationally intensive.⁴³ In the absence of a patient-specific MRI, high-quality atlas-aligned precomputed BEM and FEM human head models are available and may produce reasonably good accuracy.^{27,44}

1.8 | Scalp EEG electrodes

Although there is no consensus on the required number of scalp EEG electrodes needed for obtaining clinically relevant ESI, there is strong evidence that extending the coverage below the hairline could dramatically improve the source localization, particularly with sources from inferior surfaces of the cerebral hemispheres. An intuitively higher number of electrodes relates to a better spatial resolution of ESI and differentiation of source origin from propagation phenomena. However, a study by Lantz et al., evaluating ESI accuracy with Engel I surgical outcomes in 14 patients with drug-resistant focal epilepsy, reported the distance from the nearest surgical margin to the location of a single fit inverse model improved by approximately 2 cm from a 31- to a 63-electrode setup, with little change from a 63- to a 123-electrode setup.⁴⁵ The question

of the optimum electrode number needed for ESI may be settled for now by recommendation of the International Federation of Clinical Neurophysiology with a minimum of 25 electrodes for routine EEG recordings, extending to the inferior frontal, temporal, and occipital regions.⁴⁶

1.9 | Diagnostic yield of ESI with respect to conventional imaging tools

The primary goal of presurgical imaging evaluation is to localize the source of the seizures noninvasively, plan intracranial EEG monitoring, and optimally select the candidates who are likely to achieve a good surgical outcome. MRI, PET, and SPECT are well established in this clinical role, and there is growing evidence that ESI adds relative and additive clinical value to the standard presurgical imaging evaluation for localizing the EZ. Sperli et al. 2006 analyzed ESI performance using standard conventional EEG (19–29 electrodes) in 30 operated seizure-free children.⁴⁷ They reported that in 27 (90%) of 30 patients, ESI correctly localized the EZ at the lobar level, whereas PET and SPECT localized the EZ in 82% and 70%, respectively. They also reported ESI was correct in all extratemporal epilepsy and in 10 of 13 temporal lobe cases. Suboptimal performance of ESI in temporal lobe epilepsy (TLE) cases was explained by the lack of basal temporal lobe coverage in the study, which dramatically improved by adding HD (128 electrodes) EEG. Michel et al. reported similar findings using HD EEG, where ESI achieved localization accuracy of 93.7% at the lobar level and 79% at the sublobar level.⁴⁸ In 2011, Brodbeck et al. presented findings from a prospective study of 152 operated patients with >1 year postoperative follow-up, allowing them to compare the sensitivity and specificity of ESI against PET, MRI, and ictal SPECT for epileptic focus localization.⁵ They found ESI calculated using HD EEG (128–256 electrodes) combined with patients' MRI head models performed better than the structural MRI alone, with better sensitivity (84.1% vs. 76.3%) and markedly superior specificity (87.5% vs. 52.9%), followed by PET (sensitivity = 68.7%, specificity = 43.8%) and ictal SPECT (sensitivity = 57.7%, specificity = 46.7%). Feng and colleagues analyzed the ESI using a HD (256 electrodes) EEG of 43 patients with TLE who underwent one-stage resective surgery.⁴⁹ They reported similar findings, where ESI performed better with localization of EZ (sublobule, 91.4%; lobule, 97.1%) followed by PET (93% at lobar level) and MRI (77.1%).

Based on current literature, ≥40%–50% of patients with MRI-negative focal epilepsy will not achieve seizure freedom, despite invasive intracranial EEG monitoring.⁵⁰ ESI is an essential clinical tool in the presurgical assessment of MRI-negative cases. Brodbeck et al. 2010 analyzed ESI

in 10 operated patients with normal MRI and a postsurgical follow-up of at least 1 year.⁵¹ Five of the 10 patients had extratemporal lobe epilepsy. ESI correctly localized the epileptic focus within the resection margins in eight of 10 patients, nine of whom experienced favorable postsurgical outcomes. Rikir et al.⁵² prospectively analyzed 28 consecutive patients undergoing presurgical investigation for malformation of cortical development (MCD)-related refractory epilepsy and reported a similar observation of ESI being fully concordant with EZ in 64% and partly concordant in 36% of MRI-negative cases.

1.10 | Concordance of ESI with intracranial EEG monitoring and its effect on postsurgery outcomes

Mégevand and colleagues evaluated the localization accuracy of ESI of interictal spikes in delineating the seizure onset zone defined by subdural and depth intracranial EEG monitoring.⁵³ They calculated ESI using HD EEG (128–256 electrodes) in 38 patients with intractable focal epilepsy who underwent subsequent intracranial EEG monitoring. They reported median distance between the ESI maximum with the nearest iEEG electrode involved in the irritative zone and seizure onset zone was 15 and 17 mm, respectively, concluding that localization of interictal spikes with HD ESI correctly identified the seizure onset zone. They also reported that including the source maximum in the resected brain volume is associated with a favorable postoperative outcome, indicating that ESI of interictal spikes helps delineate the EZ. Similarly, Abdallah et al.⁵⁴ prospectively analyzed 74 patients undergoing SEEG monitoring for anatomical concordance of ESI of interictal discharges with EZ defined by SEEG. They reported ESI was completely or partly in concordance in 85% (full concordance in 13 cases and partial concordance in 50 cases); the rate of ESI full concordance with EZ was significantly higher in frontal lobe epilepsy (46%), negative MRI cases (36%), and MCD (27%).

In a study evaluating the predictive values of HD ESI in 190 patients with conventional imaging tools, Lascano et al. reported that structural MRI and HD ESI were the only two favorable outcome predictors.⁵⁵ Patients with concordant HD ESI and structural MRI findings had a 92.3% probability of a favorable surgical outcome. A recent systematic review and meta-analysis by Sharma et al.⁵⁶ evaluated the diagnostic accuracy of interictal and ictal ESI and magnetic source imaging (MSI) in epilepsy surgery, and found 25 studies on ESI that specified the diagnostic reference standard as the site of resection and the postoperative outcome (seizure-freedom). Table 1 provides a summary of the ESI studies. They reported overall accuracy was

TABLE 1 Summary of studies evaluating the ESI

Author/year	Study design	N	Source imaging	Forward model	Inverse model	Postsurgical follow-up	Final comments
Assaf and Ebersole 1999 ⁵⁷	R	75	Ictal	N/A	Fixed dipoles	2 years	ESI can determine the sublobar nature of neocortical TLE patients who could benefit from intracranial monitoring
Lantz et al. 2003 ⁴⁵	P	14	Interictal	Spherical	DSM (EPIFOCUS)	>1 year	Distance from the EEG source to the epileptic lesion was significantly smaller with 123 and 63 electrodes than with 31 electrodes
Leijten et al. 2003 ⁵⁸	P	19	Interictal	Realistic	ECD	>1 year	Better correlation was seen between EEG and ECoG findings with horizontal EEG dipole orientation and prominent neocortical spiking; these patients also had a less favorable prognosis
Michel et al. 2004 ⁴⁸	P	32	Interictal	Spherical	ECD (EPIFOCUS)	>1 year	High-resolution interictal ESI with 128 channels identified the epileptogenic area in 93% of patients with 79% accuracy of sublobar localization
Sperli et al. 2006 ⁴⁷	P	30	Interictal	Spherical	DSM	>1 year	ESI correctly localized the epileptogenic region in 90 cases and also had comparable performance with other imaging techniques in the same patients (PET, 82%; ictal SPECT, 70%)
Brodbeck et al. 2009 ²³	R	14	Interictal	Spherical	DSM (LAURA)	1 year	ESI localized the EZ in 85% of patients with large cerebral lesions
Brodbeck et al. 2010 ⁵¹	R	10	Interictal	Realistic (SMAC) model	DSM (LAURA)	1 year	ESI localized the EZ in 8 of 10 patients with MRI-negative focal epilepsy
Brodbeck et al. 2011 ⁵	P	152	Interictal	Realistic (SMAC) model	DSM (LAURA)	>1 year	With high number of electrodes (128–256) combined with patients' MRI-based head models, ESI can achieve sensitivity of 84% and specificity of 88% in localizing the EZ
Elshoff et al. 2012 ⁵⁹	P	9	Interictal	Spherical	DSM (LAURA)	½–2 years	ESI performed better than conventional EEG with fMRI BOLD signal analysis
Beniczky et al. 2013 ²²	P	42	Ictal	Spherical	DSM (LAURA)	1 year	Ictal source localization had 70% sensitivity and 76% specificity with 92% PPV for seizure freedom
Heers et al. 2014 ⁶⁰	R	21	Interictal	BEM	DSM	1 year	BOLD fMRI clusters that were spatially concordant with ESI/MSI were concordant with IEDs from invasive recordings in 8/11 patients
Kargiotis et al. 2014 ⁶¹	R	13	Interictal	Spherical	DSM	1–4 years	HD ESI was found to be more concordant than low-density ESI with resected area in seizure-free patients with TSC

(Continues)

TABLE 1 (Continued)

Author/year	Study design	N	Source imaging	Forward model	Inverse model	Postsurgical follow-up	Final comments
Mégevand et al. 2014 ⁵³	P	38	Interictal	Spherical	DSM	>1 year	Median distance from the ESI maximum to the nearest intracranial electrode involved in the SOZ was 17 mm
Rikiri et al. 2014 ⁵²	P	28	Interictal	BEM	ECD/DSM (sLORETA)	>1 year	ESI was fully concordant with the EZ in 64% and partly concordant in 36% of patients with negative MRI brain
Mazerio et al. 2015 ⁶²	R	25	Interictal	Spherical	DSM	>1 year	Presence of IEDs was associated with increased spectral range on fMRI, and ICA could improve sensitivity of fMRI data analysis without IEDs
Park et al. 2015 ⁶³	P	27	Interictal	BEM	ECD (fixed MUSIC)	>1 year	ESI localized deeper than the cortex, whereas the MSI results localized on the cortical surface; ESI findings were more concordant than MSI with ECoG data (89% vs. 80%)
Feng et al. 2016 ⁴⁹	P	43	Interictal	FDM	DSM (LORETA)	>1 year	ESI with dense array of electrodes achieved sensitivity of 91% at sublobar level; single source and sources within resection had better postsurgical outcome ($p < .05$) than multiple sources and sources outside the resection
Lascano et al. 2016 ⁵⁵	P	190	Interictal	Realistic head model	DSM (LAURA)	>12 months	MRI (OR = 10.9, $p = .004$) and HD ESI (OR = 13.1, $p = .004$) were favorable outcome predictors; concordant structural MRI and HD ESI results had 92.3% probability of favorable outcome
Beniczky et al. 2016 ⁶⁴	P	22	Ictal	FEM	DSM (phase mapping, dipole fitting, CLARA, cortical CLARA, and minimum norm)	1 year	Ictal source imaging achieved an accuracy of 73% with good agreement between different methods, but agreement between methods did not necessarily imply accuracy of localization
Li et al. 2016 ⁶⁵	P	10	Ictal	BEM	DSM (cross-frequency coupled potential signals)	1 year	Sampling at ≥ 500 Hz estimated source localized with resected region, and S_{CFRC} could effectively extract brain signals from a noisy background
Centeno et al. 2017 ⁶⁶	R	53	Interictal	–	DSM	1–5 years	Combined ESI/EEG-fMRI (91%) and ESI (83%) were more accurate than the EEG-fMRI global maxima localization (50%) of EZ

TABLE 1 (Continued)

Author/year	Study design	N	Source imaging	Forward model	Inverse model	Postsurgical follow-up	Final comments
van Mierlo et al. 2017 ⁶⁷	R	32	Interictal	Individual	DSM	>1 year	The median distance to the resection in patients with Engel class I outcome was 6.5 and 15 mm for automated spike cluster 1 and 27 and 26 mm for cluster 2, at the peak and the half-rising time of the spike, respectively
Nemtsas et al. 2017 ⁶⁸	R	14	Ictal	Locally spherical model with anatomical constraints	DSM (LORETA)	1 year	Ictal ESI localized EZ in 5/6 postoperatively seizure-free patients; high concordance was seen between IEDs and ictal ESI
Feng et al. 2018 ⁶⁹	R	43	Interictal	Individual finite difference models	DSM (LORETA)	2.5–4 years	HD ESI (256 channels) showed the best sensitivity (sublobule, 91.4%; lobule, 97.1%) and specificity (75%) for both sublobule and lobule criteria
Koren et al. 2018 ⁷⁰	R	28	Ictal	Spherical model with anatomical constraints (SMAC)	MVB		Ictal ESI in patients with TLE showed sensitivity of 92% and specificity 50%
Abdallah et al. 2017 ⁵⁴	P	74	Interictal	BEM	ECD, MUSIC, sLORETA	2 years	Full concordance of ESI with EZ was significantly higher in FLE (46%, $p = .05$), negative MRI (36%), and malformation of cortical development (27%)
Cox et al. 2021 ³⁴	P	87	Interictal–ictal	BEM	ECD/DSM (sLORETA)	1 year	Dipole and maximum distributed source to a centroid of SOZ electrodes were 30.0 and 32.5 mm, respectively; temporal lobe discharges have higher concordance rates than extratemporal discharge

Abbreviations: BEM, boundary element model; BOLD, blood oxygen level-dependent; DSM, distributed source model; ECD, equivalent current dipole; ECoG, electrocorticographic; EEG, electroencephalographic; ESI, EEG source imaging; EZ, epileptogenic zone; FEM, finite element model; FLE, frontal lobe epilepsy; fMRI, functional MRI; HD, high density; ICA, independent component analysis; IED, interictal epileptiform discharge; LAURA, local autoregressive average; MRI, magnetic resonance imaging; MSI, magnetic source imaging; MUSIC, multiple signal classification; MVB, minimum variance beamformer; N/A, not available; OR, odds ratio; P, prospective; PET, positron emission tomography; PPV, positive predictive value; R, retrospective; sLORETA, standardized low-resolution electromagnetic tomography; SOZ, seizure onset zone; SPECT, single photon emission computed tomography; TLE, temporal lobe epilepsy; TSC, tuberous sclerosis complex.

between 50% and 75% (highest for ictal ESI) and diagnostic odds ratio was between 4.02 and 7.9 (interictal ESI < interictal magnetic source imaging < ictal ESI). [Table 1](#) includes a summary of studies comparing ESI with conventional imaging and evaluating the postsurgical outcomes.

2 | CONCLUSIONS

This article covers the fundamentals behind the development of ESI and the diagnostic accuracy of ESI compared to standard conventional imaging, highlighting the importance of ESI as a valuable clinical imaging tool in the presurgical assessment of drug-resistant focal epilepsy. In approximately 20%–30% of patients with intractable epilepsy, ESI can directly influence presurgical and intracranial EEG electrode implantation planning. We also found good concordance between ESI and EZ at the sublobar level, which translates into better postsurgical outcomes; hopefully, this will encourage more level IV epilepsy centers to incorporate ESI into standard presurgical assessment.

AUTHOR CONTRIBUTIONS

All authors listed have made substantial, direct, intellectual contributions to the work, and approved it for publication.

ACKNOWLEDGMENT

None.

CONFLICT OF INTEREST

B.H.B. has a consulting agreement with Otsuka Pharmaceuticals, has received research support from Seer Medical and UNEEG Medical, and has intellectual property licensed to Cadence Neuroscience. He has also received nonfinancial research support from Medtronic, and research support from the Epilepsy Foundation and the National Institutes of Health. J.S.E. serves on Compumedics Medical Advisory Board. J.S. has no conflict of interest. We confirm that we have read the Journal's position on issues involved in ethical publication and affirm that this report is consistent with those guidelines.

ORCID

Jaysingh Singh  <https://orcid.org/0000-0003-4914-9589>
Benjamin H. Brinkmann  <https://orcid.org/0000-0002-2392-8608>

REFERENCES

- Duncan JS, Winston GP, Koepp MJ, Ourselin S. Brain imaging in the assessment for epilepsy surgery. *Lancet Neurol*. 2016;15(4):420–33.
- Knowlton RC, Elgavish RA, Bartolucci A, Ojha B, Limdi N, Blount J, et al. Functional imaging: II. Prediction of epilepsy surgery outcome. *Ann Neurol*. 2008;64(1):35–41.
- Spanaki MV, Spencer SS, Corsi M. Sensitivity and specificity of quantitative difference SPECT analysis in seizure localization. *J Nucl Med*. 1999;40(5):730–6.
- Henry TR, Van Heertum RL. Positron emission tomography and single photon emission computed tomography in epilepsy care. *Semin Nucl Med*. 2003;33(2):88–104.
- Brodbeck V, Spinelli L, Lascano AM, Wissmeier M, Vargas M-I, Vulliemoz S, et al. Electroencephalographic source imaging: a prospective study of 152 operated epileptic patients. *Brain*. 2011;134(Pt 10):2887–97.
- Wong PK. Potential fields, EEG maps, and cortical spike generators. *Electroencephalogr Clin Neurophysiol*. 1998;106(2):138–41.
- Welker W. Why does cerebral cortex fissure and fold? In: Jones EG, Peters A, editors. *Cerebral cortex*. Boston, MA: Springer; 1990. p. 3–136.
- Plummer C, Harvey AS, Cook M. EEG source localization in focal epilepsy: where are we now? *Epilepsia*. 2008;49(2):201–18.
- Mouthaan BE, Rados M, Barsi P, Boon P, Carmichael DW, Carrette E, et al. Current use of imaging and electromagnetic source localization procedures in epilepsy surgery centers across Europe. *Epilepsia*. 2016;57(5):770–6.
- Cooper R, Winter AL, Crow HJ, Walter WG. Comparison of subcortical, cortical and scalp activity using chronically indwelling electrodes in man. *Electroencephalogr Clin Neurophysiol*. 1965;18:217–28.
- Tao JX, Baldwin M, Hawes-Ebersole S, Ebersole JS. Cortical substrates of scalp EEG epileptiform discharges. *J Clin Neurophysiol*. 2007;24(2):96–100.
- Zelmann R, Lina JM, Schulze-Bonhage A, Gotman J, Jacobs J. Scalp EEG is not a blur: it can see high frequency oscillations although their generators are small. *Brain Topogr*. 2014;27(5):683–704.
- Hauk O. Keep it simple: a case for using classical minimum norm estimation in the analysis of EEG and MEG data. *Neuroimage*. 2004;21(4):1612–21.
- Grech R, Cassar T, Muscat J, Camilleri KP, Fabri SG, Zervakis M, et al. Review on solving the inverse problem in EEG source analysis. *J Neuroeng Rehabil*. 2008;5:25.
- Silva C, Maltez JC, Trindade E, Arriaga A, Ducla-Soares E. Evaluation of L1 and L2 minimum norm performances on EEG localizations. *Clin Neurophysiol*. 2004;115(7):1657–68.
- Wagner M, Fuchs M, Kastner J. Evaluation of sLORETA in the presence of noise and multiple sources. *Brain Topogr*. 2004;16(4):277–80.
- Plummer C, Wagner M, Fuchs M, Vogrin S, Litewka L, Farish S, et al. Clinical utility of distributed source modelling of interictal scalp EEG in focal epilepsy. *Clin Neurophysiol*. 2010;121(10):1726–39.
- Pascual-Marqui RD, Esslen M, Kochi K, Lehmann D. Functional imaging with low-resolution brain electromagnetic tomography (LORETA): a review. *Methods Find Exp Clin Pharmacol*. 2002;24(Suppl C):91–5.
- Worrell GA, Lagerlund TD, Sharbrough FW, Brinkmann BH, Busacker NE, Cicora KM, et al. Localization of the epileptic focus by low-resolution electromagnetic tomography in

- patients with a lesion demonstrated by MRI. *Brain Topogr*. 2000;12(4):273–82.
20. Lantz G, Michel CM, Pascual-Marqui RD, Spinelli L, Seeck M, Seri S, et al. Extracranial localization of intracranial interictal epileptiform activity using LORETA (low resolution electromagnetic tomography). *Electroencephalogr Clin Neurophysiol*. 1997;102(5):414–22.
 21. de Peralta G, Menendez R, Murray MM, Michel CM, Martuzzi R, Gonzalez Andino SL. Electrical neuroimaging based on biophysical constraints. *Neuroimage*. 2004;21(2):527–39.
 22. Beniczky S, Lantz G, Rosenzweig I, Åkeson P, Pedersen B, Pinborg LH, et al. Source localization of rhythmic ictal EEG activity: a study of diagnostic accuracy following STARD criteria. *Epilepsia*. 2013;54(10):1743–52.
 23. Brodbeck V, Lascano AM, Spinelli L, Seeck M, Michel CM. Accuracy of EEG source imaging of epileptic spikes in patients with large brain lesions. *Clin Neurophysiol*. 2009;120(4):679–85.
 24. Sohrabpour A, Lu Y, Worrell G, He B. Imaging brain source extent from EEG/MEG by means of an iteratively reweighted edge sparsity minimization (IRES) strategy. *Neuroimage*. 2016;142:27–42.
 25. Heers M, Chowdhury RA, Hedrich T, Dubeau F, Hall JA, Lina J-M, et al. Localization accuracy of distributed inverse solutions for electric and magnetic source imaging of interictal epileptic discharges in patients with focal epilepsy. *Brain Topogr*. 2016;29(1):162–81.
 26. Pellegrino G, Hedrich T, Chowdhury RA, Hall JA, Dubeau F, Lina J-M, et al. Clinical yield of magnetoencephalography distributed source imaging in epilepsy: a comparison with equivalent current dipole method. *Hum Brain Mapp*. 2018;39(1):218–31.
 27. Fuchs M, Kastner J, Wagner M, Hawes S, Ebersole JS. A standardized boundary element method volume conductor model. *Clin Neurophysiol*. 2002;113(5):702–12.
 28. Plummer C, Vogrin SJ, Woods WP, Murphy MA, Cook MJ, Liley DTJ. Interictal and ictal source localization for epilepsy surgery using high-density EEG with MEG: a prospective long-term study. *Brain*. 2019;142(4):932–51.
 29. Kural MA, Jing J, Fürbass F, Perko H, Qerama E, Johnsen B, et al. Accurate identification of EEG recordings with interictal epileptiform discharges using a hybrid approach: artificial intelligence supervised by human experts. *Epilepsia*. 2022;63:1064–73.
 30. Baroumand AG, van Mierlo P, Strobbe G, Pinborg LH, Fabricius M, Rubboli G, et al. Automated EEG source imaging: a retrospective, blinded clinical validation study. *Clin Neurophysiol*. 2018;129(11):2403–10.
 31. Heers M, Böttcher S, Kalina A, Katletz S, Altenmüller D-M, Baroumand AG, et al. Detection of interictal epileptiform discharges in an extended scalp EEG array and high-density EEG—a prospective multicenter study. *Epilepsia*. 2022;63(7):1619–29.
 32. van Mierlo P, Vorderwülbecke BJ, Staljanssens W, Seeck M, Vulliémou S. Ictal EEG source localization in focal epilepsy: review and future perspectives. *Clin Neurophysiol*. 2020;131(11):2600–16.
 33. Mosher JC, Baillet S, Leahy RM. EEG source localization and imaging using multiple signal classification approaches. *J Clin Neurophysiol*. 1999;16(3):225–38.
 34. Cox BC, Danoun OA, Lundstrom BN, Lagerlund TD, Wong-Kissel LC, Brinkmann BH. EEG source imaging concordance with intracranial EEG and epileptologist review in focal epilepsy. *Brain Commun*. 2021;3(4):fcb278.
 35. Henderson CJ, Butler SR, Glass A. The localization of equivalent dipoles of EEG sources by the application of electrical field theory. *Electroencephalogr Clin Neurophysiol*. 1975;39(2):117–30.
 36. Cuffin BN, Schomer DL, Ives JR, Blume H. Experimental tests of EEG source localization accuracy in spherical head models. *Clin Neurophysiol*. 2001;112(1):46–51.
 37. Yvert B, Bertrand O, Thévenet M, Echallier JF, Pernier J. A systematic evaluation of the spherical model accuracy in EEG dipole localization. *Electroencephalogr Clin Neurophysiol*. 1997;102(5):452–9.
 38. Baillet S, Riera JJ, Marin G, Mangin JF. Evaluation of inverse methods and head models for EEG source localization using a human skull phantom. *Phys Med*. 2001;46:77–96.
 39. Fuchs M, Wagner M, Kastner J. Boundary element method volume conductor models for EEG source reconstruction. *Clin Neurophysiol*. 2001;112(8):1400–7.
 40. Vatta F, Meneghini F, Esposito F, Minin S, Di Salle F. Realistic and spherical head modeling for EEG forward problem solution: a comparative cortex-based analysis. *Comput Intell Neurosci*. 2010;14:972060.
 41. Akalin Acar Z, Makeig S. Effects of forward model errors on EEG source localization. *Brain Topogr*. 2013;26(3):378–96.
 42. Dannhauer M, Lanfer B, Wolters CH, Knösche TR. Modeling of the human skull in EEG source analysis. *Hum Brain Mapp*. 2011;32(9):1383–99.
 43. Vorwerk J, Clerc M, Burger M, Wolters CH. Comparison of boundary element and finite element approaches to the EEG forward problem. *Biomed Tech (Berl)*. 2012;57(Suppl 1). <https://doi.org/10.1515/bmt-2012-4152>
 44. Huang Y, Parra LC, Haufe S. The New York head—a precise standardized volume conductor model for EEG source localization and tES targeting. *Neuroimage*. 2016;140:150–62.
 45. Lantz G, Grave de Peralta R, Spinelli L, Seeck M, Michel CM. Epileptic source localization with high density EEG: how many electrodes are needed? *Clin Neurophysiol*. 2003;114(1):63–9.
 46. Seeck M, Koessler L, Bast T, Leijten F, Michel C, Baumgartner C, et al. The standardized EEG electrode array of the IFCN. *Clin Neurophysiol*. 2017;128(10):2070–7.
 47. Sperl F, Spinelli L, Seeck M, Kurian M, Michel CM, Lantz G. EEG source imaging in pediatric epilepsy surgery: a new perspective in presurgical workup. *Epilepsia*. 2006;47(6):981–90.
 48. Michel CM, Lantz G, Spinelli L, De Peralta RG, Landis T, Seeck M. 128-channel EEG source imaging in epilepsy: clinical yield and localization precision. *J Clin Neurophysiol*. 2004;21(2):71–83.
 49. Feng R, Hu J, Pan L, Wu J, Lang L, Jiang S, et al. Application of 256-channel dense array electroencephalographic source imaging in presurgical workup of temporal lobe epilepsy. *Clin Neurophysiol*. 2016;127(1):108–16.
 50. Jayakar P, Dunoyer C, Dean P, Ragheb J, Resnick T, Morrison G, et al. Epilepsy surgery in patients with normal or nonfocal MRI scans: integrative strategies offer long-term seizure relief. *Epilepsia*. 2008;49(5):758–64.

51. Brodbeck V, Spinelli L, Lascano AM, Pollo C, Schaller K, Vargas MI, et al. Electrical source imaging for presurgical focus localization in epilepsy patients with normal MRI. *Epilepsia*. 2010;51(4):583–91.
52. Rikir E, Koessler L, Gavaret M, Bartolomei F, Colnat-Coulbois S, Vignal J-P, et al. Electrical source imaging in cortical malformation-related epilepsy: a prospective EEG-SEEG concordance study. *Epilepsia*. 2014;55(6):918–32.
53. Mégevand P, Spinelli L, Genetti M, Brodbeck V, Momjian S, Schaller K, et al. Electric source imaging of interictal activity accurately localises the seizure onset zone. *J Neurol Neurosurg Psychiatry*. 2014;85(1):38–43.
54. Abdallah C, Maillard LG, Rikir E, Jonas J, Thiriaux A, Gavaret M, et al. Localizing value of electrical source imaging: frontal lobe, malformations of cortical development and negative MRI related epilepsies are the best candidates. *Neuroimage Clin*. 2017;16:319–29.
55. Lascano AM, Perneger T, Vulliemoz S, Spinelli L, Garibotto V, Korff CM, et al. Yield of MRI, high-density electric source imaging (HD-ESI), SPECT and PET in epilepsy surgery candidates. *Clin Neurophysiol*. 2016;127(1):150–5.
56. Sharma P, Seeck M, Beniczky S. Accuracy of interictal and ictal electric and magnetic source imaging: a systematic review and meta-analysis. *Front Neurol*. 2019;10:1250.
57. Assaf BA, Ebersole JS. Visual and quantitative ictal EEG predictors of outcome after temporal lobectomy. *Epilepsia*. 1999;40(1):52–61.
58. Leijten FSS, Huiskamp G-JM, Hilgersom I, Van Huffelen AC. High-resolution source imaging in mesiotemporal lobe epilepsy: a comparison between MEG and simultaneous EEG. *J Clin Neurophysiol*. 2003;20(4):227–38.
59. Elshoff L, Groening K, Grouiller F, Wiegand G, Wolff S, Michel C, et al. The value of EEG-fMRI and EEG source analysis in the presurgical setup of children with refractory focal epilepsy. *Epilepsia*. 2012;53(9):1597–606.
60. Heers M, Hedrich T, An D, Dubeau F, Gotman J, Grova C, et al. Spatial correlation of hemodynamic changes related to interictal epileptic discharges with electric and magnetic source imaging. *Hum Brain Mapp*. 2014;35(9):4396–414.
61. Kargiotis O, Lascano AM, Garibotto V, Spinelli L, Genetti M, Wissmeyer M, et al. Localization of the epileptogenic tuber with electric source imaging in patients with tuberous sclerosis. *Epilepsy Res*. 2014;108(2):267–79.
62. Maziero D, Sturzbecher M, Velasco TR, Rondinoni C, Castellanos AL, Carmichael DW, et al. A comparison of independent component analysis (ICA) of fMRI and electrical source imaging (ESI) in focal epilepsy reveals misclassification using a classifier. *Brain Topogr*. 2015;28(6):813–31.
63. Park CJ, Seo JH, Kim D, Abibullaev B, Kwon H, Lee YH, et al. EEG source imaging in partial epilepsy in comparison with presurgical evaluation and magnetoencephalography. *J Clin Neurol*. 2015;11(4):319–30.
64. Beniczky S, Rosenzweig I, Scherg M, Jordanov T, Lanfer B, Lantz G, et al. Ictal EEG source imaging in presurgical evaluation: high agreement between analysis methods. *Seizure*. 2016;43:1–5.
65. Li C, Jacobs D, Hilton T, Campo MD, Chinvarun Y, Carlen PL, et al. Epileptogenic source imaging using cross-frequency coupled signals from scalp EEG. *IEEE Trans Biomed Eng*. 2016;63(12):2607–18.
66. Centeno M, Tierney TM, Perani S, Shamshiri EA, St Pier K, Wilkinson C, et al. Combined electroencephalography-functional magnetic resonance imaging and electrical source imaging improves localization of pediatric focal epilepsy. *Ann Neurol*. 2017;82(2):278–87.
67. van Mierlo P, Strobbe G, Keereman V, Birot G, Gadeyne S, Gschwind M, et al. Automated long-term EEG analysis to localize the epileptogenic zone. *Epilepsia Open*. 2017;2(3):322–33.
68. Nemtsas P, Birot G, Pittau F, Michel CM, Schaller K, Vulliemoz S, et al. Source localization of ictal epileptic activity based on high-density scalp EEG data. *Epilepsia*. 2017;58(6):1027–36.
69. Feng R, Hu J, Wu J, Lang L, Ma C, Sun B, et al. Accurate source imaging based on high resolution scalp electroencephalography and individualized finite difference head models in epilepsy pre-surgical workup. *Seizure*. 2018;59:126–31.
70. Koren J, Gritsch G, Pirker S, Herta J, Perko H, Kluge T, et al. Automatic ictal onset source localization in presurgical epilepsy evaluation. *Clin Neurophysiol*. 2018;129(6):1291–9.

How to cite this article: Singh J, Ebersole JS, Brinkmann BH. From theory to practical fundamentals of electroencephalographic source imaging in localizing the epileptogenic zone. *Epilepsia*. 2022;63:2476–2490. <https://doi.org/10.1111/epi.17361>